ELECTROCHEMICAL MASS TRANSFER IN ACTIVE AND PASSIVE FLUIDIZED BEDS

By

L. M. Kovács

Department of Chemical Technology, Technical University, Budapest

Received December 5, 1979

Presented by Prof. Dr. I. Szebényi

In the last decade there were several attempts to use particulate electrodes with higher surface area in unit volume of cell to electrochemically react dilute solutions. Reactions may include metal deposition such as Cu, Pb, Hg, Sb or Ag from dilute solutions of these ions, changing the valence of the ions or causing complete chemical destruction by electrode reactions of materials as cyanide or phenol. This type of electrochemical reactors suits electro-organic synthesis as well [1]. The main developments in design of high specific surface electrodes were those by Goodrodge [2] inventing and applying fluidized bed cell, and by Ibl [3] inventing the so-called "Swiss roll cell".

The effectiveness of different electrochemical reactors can be compared by the specific electrode area a_p and the space time yield Y_{st}. Let us compare some different electrochemical cells according to F. Beek's data collection [4] on the basis of a_p and Y_{st} in Table 1.

Table 1

Comparison of different cells

Type of cell	a_p (cm^{-1})	Y_{st} (mol h^{-1}cm^{-3})
Filter press	0.3 — 1.7	0.12 — 0.68
Capillary gap	1 — 5.0	0.4 — 2.0
Rotating or wiped electrodes	0.1	0.04
Packed bed	10 — 50	4 — 20
Fluidized bed	20 — 100	8 — 40

The advantages of packed bed and fluidized bed cells are obvious from the table. The superficial surface area a_p — defined as the electrode surface in unit volume of cell — is by about two orders higher in the case of packed beds and fluidized beds. According to this the specific productivity (the so-called space time yield defined as the amount produced by unit volume of cell in unit time)

of the high specific surface area packed-bed and fluidized-bed electrochemical reactors is higher by about two orders as well.

Illustrating this difference between flat-plate, inert-bed, and active-bed electrodes from our measurements, the limiting current by unit diaphragm area as a function of superficial velocity of solution for different-type cells is shown in Fig. 1.

The packed and fluidized beds are widely used in chemical engineering for mass-transfer-controlled processes and during decades great many useful data have been accumulated in this field likely of use in electrochemical engineering.

The recent work has two aims. One is to compare the advantages and disadvantages of three different type electrochemical cells; the other is to com-
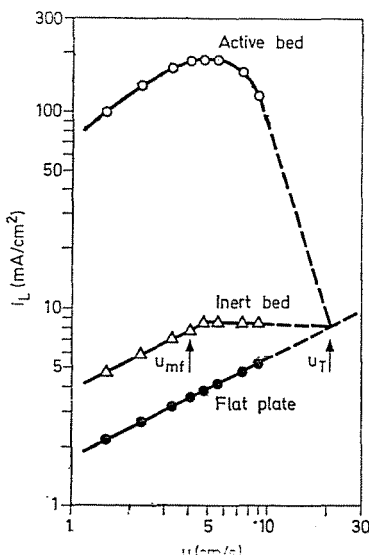
Fig. 1. The variation of limiting current density across unit diaphragm area as a function of superficial solution velocity for different types of cells
+ flat-plate; △ inert-bed; ○ active-bed

pare the mass transfer phenomena between electrochemical and non-electrochemical units. It is important to see how non-electrochemical mass transfer data can be applied for designing electrochemical reactors with high specific surface electrodes.

The mass transfer in an electrochemical system is due to migration, diffusion and convection. Near the electrode surface in the diffusion sublayer the convection can be neglected and using supporting electrolyte in a high excess the migration term becomes negligible. The mass flux in the diffusion sublayer can be written in two-dimensional form:

$$N_i = - D_i \left(\frac{\partial c_i}{\partial y}\right)_{y=0} = D_i \frac{c_b - c_s}{\delta} . \tag{1}$$

In dilute solutions generally the mass transfer controls the overall reaction rate. When the reacting ion concentration at the electrode surface becomes zero ($c_s = 0$) the limiting current is reached. From limiting current density the mass transfer coefficient can be calculated as follows:

$$k = \frac{i_L}{ZFc_b}.$$ (2)

In the present work the mass transfer coefficients were measured in the case of plane plate and fluidized bed cathode during the electrowinning of copper from an acidified dilute solution.

Experimental

A perspex cell with rectangular geometry has been used to deposit copper from acidified aqueous solution, containing 3 g/l of copper and 135 g/l sulfuric acid as nominal composition. Both chemicals are purum grade. The cross section
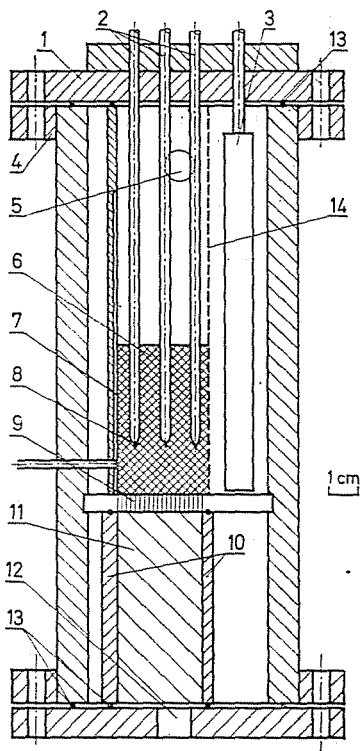
Fig. 2. The cross-section of electrolyzer

1. lid; 2. Luggin capillaries; 3. anode; 4. flange; 5. outlet; 6. bed of spheres; 7. cathode; 8. copper wire; 9. supporting plate; 10. perspex wall; 11. liquid distributor; 12. inlet; 13. gaskets; 14. diaphragm

of the electrolyzer is shown in Fig. 2. The cathode was made of copper and the anode material was lead. The cathode and anode chamber were separated by a porous PVC diaphragm. The dimensions of the cathode compartment were: 3 cm in the direction of current flow (thickness), 5 cm wide and 10 cm in height. Under the cathode chamber there was a 7 cm high compartment filled with 5 mm diam. glass beads to make uniform solution velocity distribution.

The electrolyte inlet was at the bottom, while the outlet was at the top of the cell. There were some Luggin capillaries for potential distribution measurements in the bed.
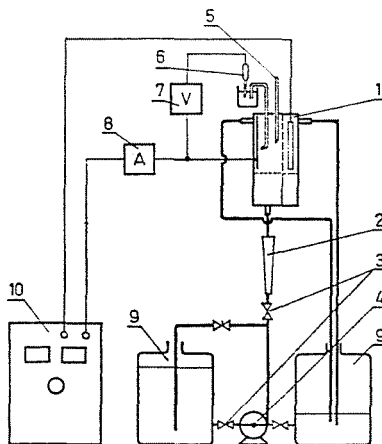
Fig. 3. The flow circuit of the apparatus
1. electrolyzer; 2. rotameter; 3. valves; 4. pump; 5. thermometer; 6. kalomel electrode; 7. electronic voltmeter; 8. ammeter; 9. reservoirs; 10. power supply

The flow circuit of the apparatus is shown in Fig. 3. The solution was circulated by a pump from a tank across a flowmeter to the cell and collected in a reservoir. The direct current was supplied by a TCO 12/100 type rectifier. The cathode potential was measured by a TR 1456 type electronic voltmeter and the current passed through the cell was measured by a LDAV-1 type ammeter. Cathode potential and potential distribution measurements were made by means of saturated calomel electrodes via Luggin capillaries. The physical data of solution were adopted from CARBIN and GABE [5]. The copper concentration of the solution was measured repeatedly by d.c. polarography.

Mass transfer on the plane plate electrode

To compare cell capacities, first the mass transfer in the plane plate was investigated. The limiting current was measured at different flow rates and the mass transfer was calculated from the limiting current. From mass transfer

coefficients, linear velocity of solution and other physical data, a dimensionless so-called criterial equation was formed for the sake of comparison. According to SKELLAND [6] the mass transfer in an ideal flat plate can be characterized as:

$$\text{Sh} = \frac{k \cdot L}{D} = 0{,}646 \, \text{Re}_L^{1/2} \, \text{Sc}^{1/3} \, . \tag{4}$$

In this study the solution velocity varied from 1.5 to 10.5 cm/s while the length of the electrode varied from 1 to 10 cm. From the measured limiting current a criterial equation was established in the form of Eq. (4):

$$\text{Sh} = \frac{k \cdot L}{D} = 4.6 \, \text{Re}_L^{0.5} \, \text{Sc}^{1/3} \, . \tag{5}$$

In recent measurements of copper deposition on copper cathode at limiting current, the powers of Reynolds and Schmidt numbers are the same but the constant differs considerably from that in Skelland's analytically derived equation. The main reason is that near the limiting current, the deposition is porous, with a surface nearly one order higher for mass transfer than the ideally smooth surface.

Mass transfer of flat electrode with glass beads

Flat electrode measurements showed the mass transfer rate to increased upon increasing the solution velocity. When glass beads were put into the cathode chamber the linear velocity increased because the solution could only flow in the voids of glass beads. When the solution velocity increased over the minimum fluidization velocity the glass beads got fluidized giving an additional kinetic energy to mix the diffusional layer and promote mass transfer. 3, 4 and 5 mm nominal diameter glass beads were used in packed- and fluidized-bed form. The results were given in the form usual in mass transfer between flat wall and fluidized particles [7]:

$$\frac{k}{u} \, \varepsilon \, \text{Sc}^{2/3} = C \left(\frac{u d_p}{\nu (1 - \varepsilon)} \right)^{-m} \, . \tag{6}$$

Table 2 is a comparison between data obtained by different authors according to Eq. (6).

Table 2 shows powers m obtained in this work to be somewhat lower than average — (except Ziegler data). The mass transfer rate is seen to be somewhat higher in the case of metal deposition than in other electrochemical redox processes, attributed to the porosity of metal deposit.

Table 2

The C and m values from data obtained by different authors for inert particles according to Eq. (6)

Author	C	m	$\dfrac{u\,d_p}{v(1-\varepsilon)}$	Sc	ε
Fix bed (liq)					
THOENES [8]	0.7±0.1	0.40	50—5000	0.9—3700	0.35—0.45
KRISHNA [9]	0.8 (1—)	0.38	3—6600	256—1150	0.37—0.57
RAMANA RAO [10]	0.97	0.40	9—6000	720—1060	0.41—0.64
Fluidized bed (liq)					
JOTTRAND [11]	0.6±0.1	0.37	2—2800	1440	0.47—0.9
JAGANNADHARAJU [12]	0.43±0.05	0.38	200—24 000	1300	0.4—0.9
KRISHNA [13]	0.43±0.05	0.38	150—5000	1300	0.5—0.9
COEURET [14]	1.2±0.1	0.52	6—200	1250	0.45—0.85
CARBIN [5]	1.24	0.57	0.1—70	753	0.45—0.86
ZIEGLER [15] (gas)	0.07	0.0	300—12 000	2.57	0.5—0.95
Present work	0.56±0.1	0.33	80—1050	1260	0.37—0.64

The mass transfer of copper coated glass beads

The capacity of an electrochemical cell is greatly increased by filling the electrode chamber with electrically conducting particles increasing the working electrode surface. Study of the mass transfer of copper coated glass beads showed the limiting current not to be reached uniformly throughout the bed, because of the nonuniformity of potential distribution. To approach limiting current, the potential had been increased until hydrogen evolution started. This current was taken as the limiting one, in calculating mass transfer rate. To overcome this potential nonuniformity problem, measurements have been done to examine the mass transfer of a single copper sphere, in a bed of uniform diameter glass beads.

During active bed measurements copper coated glass beads were used. 3 mm diam. glass particles were coated with copper by a chemical method according to GOODRIDGE [16]. The cathode chamber was filled with these particles with the following dimensions: thickness (in direction of current flow): 30 mm, width: 50 mm, height (in direction of solution flow) at rest: 50 mm.

From measured data, a dimensionless equation was established (similar to Eq. 6) for the active-bed mass transfer.

The mass transfer between fluids and fluidized solid particles was studied by BEEK [17] who collected several data of mass transfer, in the case of solid-liquid and solid-gas fluidization and packed bed as well. His approach seems to

be of general validity. Our measurements were compared to data collected by Beek. For comparison, data are shown in Table 3. Beek's collected data have a relatively high deviation in the form of Eq. (6). To decrease this deviation Beek introduced a modification.

Table 3

The C and m values in Eq. (6) from data obtained by different authors for active particles

Author	C	m	Re	Sc
THOENES [18]	1.24 ± 0.25	0.55	50—500	800—1300
CHU [19]	1.5	0.54	15—110	1100
BEEK [17]	0.85 ± 0.25	0.38	15—5000	0.5—2000
FLEISCHMANN [21]	1.52	0.5	2—30	670
Present work				
single sphere	0.97 ± 0.08	0.45	70—700	1260
active-bed	0.33 ± 0.03	0.33	70—700	1260

By treating the porosity as a separate function according to Eq. (7):

$$\frac{k_p}{u} \varepsilon \, \mathrm{Sc}^{2/3} = f(\varepsilon) \left(\frac{u d_p}{\nu}\right)^{-m}. \tag{7}$$

Recalculating the data (collected by Beek) according to Eq. (7) the following two equations were obtained:

$$\frac{k_p}{u} \varepsilon \, \mathrm{Sc}^{2/3} = (0.81 \pm 0.05) \left(\frac{u d_p}{\nu}\right)^{-0.5} \tag{8}$$

if $5 < \dfrac{u d_p}{\nu} < 500$

$$\frac{k_p}{u} \varepsilon \, \mathrm{Sc}^{2/3} = (0.6 \pm 0.1) \left(\frac{u d_p}{\nu}\right)^{-4.43} \tag{9}$$

if $50 < \dfrac{u d_p}{\nu} < 2000$.

According to Eqs (8) and (9) the recent data are much closer to Beek's data collection.

Comparison of recent measurements is shown in Fig. 4. Eqs (7) and (8) are seen to suit calculation of mass transfer coefficients for active-bed electro-chemical systems. The mass transfer of a single sphere is a little higher and that of packed-bed is somewhat lower than expected from Eq. (9).
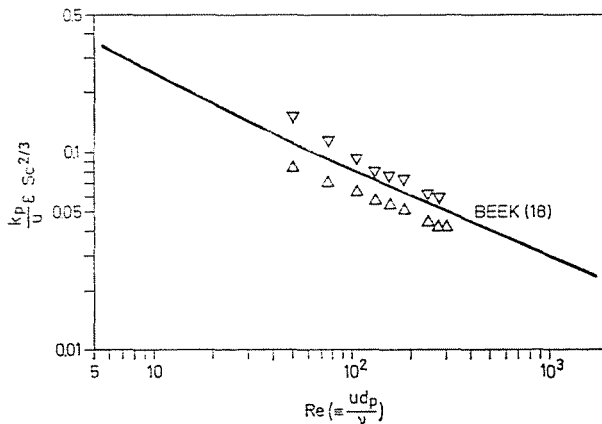
Fig. 4. The mass transfer of active spheres, compared to Beek's data collection
▽ single sphere; △ active-bed

The reason is the potential nonuniformity throughout the bed. In the case of a single sphere the potential distribution around the sphere is quite uniform, so the limiting current is reached at any part of the sphere. The potential distribution between electrode and electrolyte is less uniform in the case of porous or active packed-bed electrodes. The potential uniformity can be improved by fluidizing the bed or to put inert particles into the bed of active particles as OGUMI [21] has suggested.

The potential distribution measurements of active bed electrode

In the case of still bed or porous electrode the particles of electrode are practically of the same potential, because the resistivity of the metal lattice can be neglected beside that of the solution. The potential difference between particles and solution is rather high at the diaphragm, while small at the feeder electrode. This causes large nonuniformity of potential and current distribution as well.

In the case of fluidized bed of active (conductive) particles the potential distribution becomes more uniform, because current can flow between particles during collisions only. In this way the potential of the particles also changes, making the potential distribution more uniform.

The active-bed arrangement used in this study, and the typical potential distribution are shown in Fig. 5. The active bed is in between feeder electrode and diaphragm. The solution flows (as shown in the figure) perpendicularly to the current I. On the figure the potential variation of solution Φ_s, the particles, metal, in the case of fluidized bed Φ_m and of packed bed Φ_m.
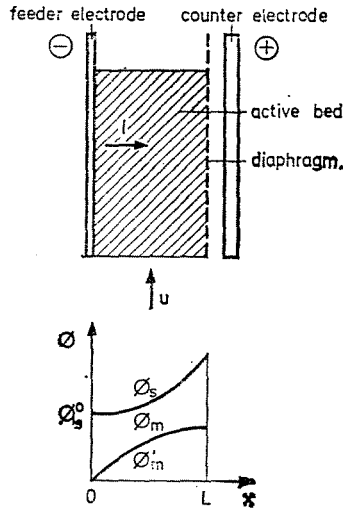
Fig. 5. The used arrangement of packed bed and a typical potential distribution

In the case of packed bed electrode the current and potential distribution is determined by several parameters. Using microkinetics to model the system, the approach becomes very difficult. It seemed to be more practical to study the potential distribution quantitatively, on the basis of a macrokinetic model. This takes the main parameters of the system into account but does not deal with such macrokinetical parameters in detail as the capacity of the double layer, the collision time of the spheres etc. as was done by FLEISCHMANN [20]. To make a simple mathematical model for potential distribution, the variation perpendicular to the current flow can be neglected, and the variation is only examined in the current flow.

The potential can be assumed to vary continuously both in the solution and in the metal phase, proportional to the ohmic potential drop. Applying Ohm's law for the metal phase:

$$i = \varrho_m^{-1} \frac{d\Phi_m}{dx}. \tag{10}$$

Ohm's law for the continuous solution phase:

$$i = - \varrho_s^{-1} \frac{d\Phi_s}{dx} \tag{11}$$

$$\text{where } \varrho_s = \varrho_s^0 \varepsilon^{3/2} \tag{12}$$

The differential equation has to take into account that the current flows in unit volume between phases numerically equal the charge transferred from electrode to solution, determined by the polarization equation that can be written an electrode length dx as follows:

$$di = a_p f(\Phi, c) dx \tag{13}$$

where $\Phi = \Phi_m - \Phi_s$ and c is the concentration of reacting species.
Combining Eqs (10), (11) and (13) the two basic differential equations are obtained:

$$\varrho_m^{-1} \frac{d^2\Phi_m}{dx^2} - a_p f(\Phi, c) = 0 \tag{14}$$

$$\varrho_s^{-1} \frac{d^2\Phi_m}{dx^2} + a_p f(\Phi, c) = 0. \tag{15}$$

FLEISCHMANN [20] has solved these equations for number of special cases of activation polarization and diffusion controlled processes.

In recent work the equation has been solved for cell configuration seen in Fig. 5.

The boundary conditions were:

$$\text{at } x = 0; \quad \Phi_s = \Phi_s = \Phi; \ \Phi_m = 0 \tag{16}$$

$$x = L; \ \frac{d\Phi_s}{dx} = \frac{d\Phi}{dx}; \ \frac{d\Phi_m}{dx} = 0 \tag{17}$$

$$x = 0; \ \frac{d\Phi_s}{dx} = 0; \quad \frac{d\Phi_m}{dx} = \frac{d\Phi}{dx}. \tag{18}$$

For diffusion controlled electrochemical processes the polarization equation can be written as:

$$f(\Phi, c) = nFc(x) \frac{D}{\delta_d} \tag{19}$$

where $c(x)$ is the concentration of reacting species. During recent measurements, the variation of concentration in direction x (current flow) may be neglected. So Eqs (14), (15) simplify to Eqs (20) and (21):

$$\frac{d^2\Phi_m}{dx^2} + A_1 = 0 \tag{20}$$

$$\frac{d^2\Phi_s}{dx^2} - A_2 = 0 \tag{21}$$

where

$$A_1 = \frac{a_p \varrho_m nFD c_b}{\delta_d} \tag{22}$$

$$A_2 = \frac{a_p \varrho_s nFD c_b}{\delta_d}. \tag{23}$$

Solving Eqs (20) and (21) with boundary conditions (16), (17) and (18) results for the potential variations in:

$$\Phi_m = -\frac{A_1}{2} x^2 + A_1 L x \tag{24}$$

$$\Phi_s = \Phi_s^0 + \frac{A_2}{2} x^2. \tag{25}$$

For correlating results obtained in the case of copper deposit potential measurements, A_1 and A_2 are calculated in a WANG 2200 computer. The values are shown in Table 4.

<div align="center">Table 4</div>

<div align="center">The physical parameters and equation constants calculated from measured data</div>

u cm/s	ε	$k \cdot 10^3$ cm/s	A_1 mV/cm²	ϱ_m ohm/cm	K_m (ohm/cm)⁻¹	A_2 mV/cm²	ϱ_s ohm/cm	K_s (ohm/cm)⁻²	φ_s mV	a_{p_1} cm
1.5	0.37	2.9	—	—	—	119	3.44	0.29	84	12.5
2.3	0.37	4.0	—	—	—	106	2.22	0.45	78	12.5
3.2	0.37	4.7	—	—	—	102	1.8	0.56	64	12.5
4.0	0.37	5.2	—	—	—	97.4	1.56	0.64	57	12.5
4.7	0.37	5.5	—	—	—	84.0	1.39	0.72	53	12.5
5.2	0.43	5.6	8.0	0.13	7.4	82.0	1.33	0.75	70	11.4
6.3	0.48	5.6	16.3	0.29	3.4	65.7	1.17	0.85	125	10.4
7.1	0.52	5.5	22.9	0.45	2.2	50.4	1.09	0.81	175	9.6
8.0	0.55	5.5	31.5	0.66	1.5	47.8	1.0	1.0	210	9.0
8.8	0.58	5.4	39.8	0.81	1.1	40.7	0.99	1.07	250	8.4

Potential distribution measurement

The variation of potential in direction of current flow was measured by a method similar to that developed by Goodridge [21]. This method suits to measure the values Φ_m and Φ_s nearly at the same place. The arrangement of potential distribution measurements with probe places is shown in Fig. 6. The probe ends were placed by about 15 mm above the beads' support. The obtained data are shown in Figs 7, 8 and 9.

Figure 7 shows variation of the solution potential Φ_m in direction of current flow, for different solution velocities. The potential of metal phase did not changed because of the packed (still) bed. Figure 8 shows the potential variations of solution (Φ_s) and metal (Φ_m) phase in the case of fluidized bed of active particles for different bed expansions. In both cases the current density
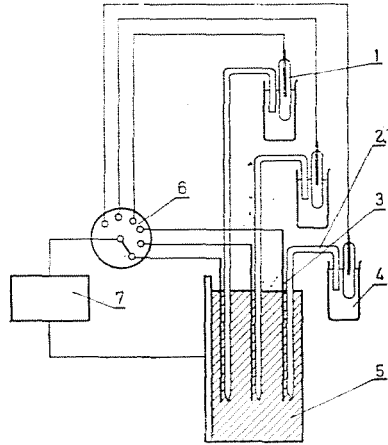
Fig. 6. The circuit for potential distribution measurements
1. kalomel electrodes; 2. Luggin capillaries; 3. copper wire; 4. saturated KCl solution; 5. active bed; 6. selector switch; 7. electronic voltmeter
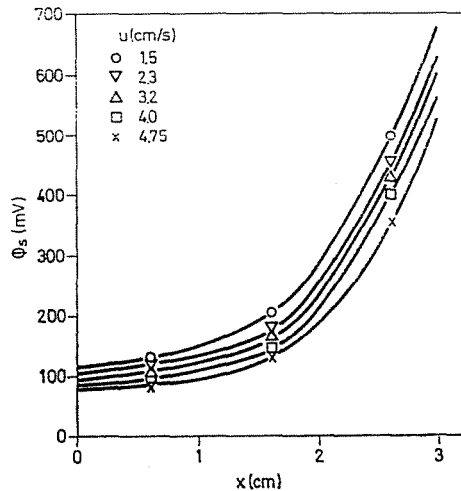
Fig. 7. The potential variation of solution in the case of active packed bed

was $1000 \, A/m^2$ of diaphragm area. Figure 9 shows the potential difference $(\Phi = \Phi_s - \Phi_m)$ variation in the case of a fluidized bed for different expansions.

The activity of a packed bed is the highest at the diaphragm. The potential greatly differs between the cathode feeder and the diaphragm. Increasing the velocity, the potential necessary to pass a current density $1000 \, A/m^2$ of diaphragm area decreases.

Further increasing the solution velocity the bed begins to be fluidized.

The most typical parameter of a fluidized bed is the bed expansion. Increasing the expansion of the fluidized bed, the potential difference decreases, the potential distribution is more uniform. This is explained by that increasing the bed expansion (by increasing velocity) increases the solution conductivity and de
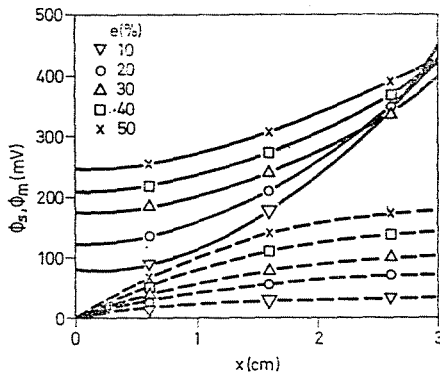
Fig. 8. The potential distribution in the case of active fluidized bed
— Φ_s; – – – Φ_m
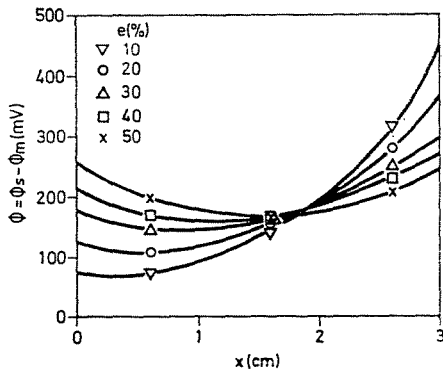
Fig. 9. The variation of potential in the case of active fluidized bed

creases the overall conductivity of metal phase. At about 50% bed expansion ($\mu \simeq 9$ cm/s) the conductivities of solution phase and metal phase become equal.

The variation of the conductivities of the two phases is shown in Fig. 10. According to this the potential distribution is seen to be in Fig. 9 the most uniform at 50% porosity and identical conductivities of the two phases. The physical parametres and equation constants calculated from potential distribution measurement data have been compiled in Table 4.
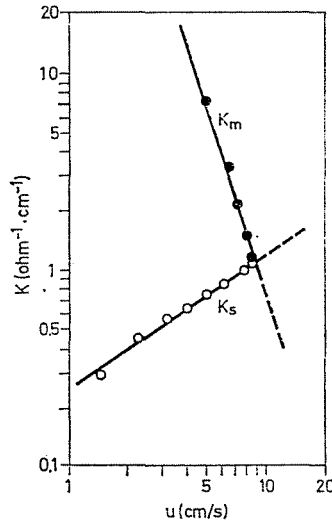
Fig. 10. The variation of conductivity of solution and metal phase as a function of solution velocity

Some design problems

The high specific surface electrodes can be used to treat dilute solutions where the controlling step is mass transfer.

The plane plate cells are advantageous if the current density is higher than 0.1 A/m^2.

If the current density is smaller than this, it seems to be better to use high specific surface area electrodes. In present work, the current density obtained in the case of a plane electrode was 0.004 A/m^2. Applying 3 mm diam. copper coated glass beads in 30 mm thickness, the current density — across the diaphragm — increased to 0.2 A/m^2.

The diaphragm current density can be increased expediently up to 1 A/m^2. It has been proved that mass transfer data of other, similar but not electrochemical systems can be used for electrochemical mass transfer of diffusion-controlled processes. For this purpose Eqs (8), (9) can be used.

Schaling up a cell with a three-dimensional electrode, the most sensitive size is the bed thickness x along the current flow. To examine this parameter, research has to be done.

For an approximate design, ARMSTRONGS' [22] equation can be used successfully:

$$x_{max} = \sqrt{\frac{2 K_s \Delta \Phi}{a_p i_L}} \, . \tag{26}$$

This equation gives the allowed bed thickness for a given (allowed) potential difference $\Delta\Phi$. The other two dimensions may be increased more freely. Restrictions are the nonuniformity of fluidization and the mechanical strength of diaphragm.

Design of an electrochemical cell of this type has to meet the following requirements:

— good mass and heat transfer: they can be calculated from Eqs (8), (9);
— uniform potential distribution: it can be obtained from $x \leq x_{max}$ calculated from Eq. (26);
— small ohmic drop: possible with relatively high K_s and K_m;
— simple operation and maintenance;
— continuous service;
— possibilities to work at elevated pressures and temperatures.

These last three requirements can be met by using techniques as usual in other chemical engineering equipment.

To use three-dimensional fluidized electrodes the advantages and disadvantages of these cell types have to be taken into account.

The advantages are:

— The working surface of the cell is considerably increased compared to that of flat electrodes.
— The fluidization increases the heat and mass transfer.
— The fluidized electrode can be continuously taken out and in for continuous movement of solid phase.

The disadvantages are:

— The nonuniformity in potential distribution (to be reduced by proper process parameters).
— The need for more accurate process control.

Acknowledgment

Summary

Experimental measurements are reported on for the study of mass transfer of plane-plate, inert-bed and active-bed electrochemical cells, using copper deposition from acidified dilute copper solution.

The mass transfers by different cells were compared to data obtained by different authors. The mass transfer in a diffusion-controlled electrochemical reaction can be calculated from mass transfer equations obtained for similar but not electrochemical systems. The potential distribution has been also measured in the case of a bed of copper-coated glass beads. The

potential distribution of a packed bed is highly non-uniform, while in the case of a fluidized bed the uniformity of potential distribution can be increased by increasing the bed expansion up to 50%.

Finally, some hints are given on designing cells with high specific surface electrodes, on the advantages and disadvantages of these cell types.

List of symbols

A	constant in differential equation	$V L^{-2}$
a_p	superficial surface area of particles	L^{-1}
c	concentration of reacting species	$M L^{-3}$
c_b	bulk concentration	$M L^{-3}$
C	constants of criterial equations	—
D	diffusivity of solution	$L^2 T^{-1}$
d_p	diameter of particles (spheres)	L
e	bed expansion $(h/h_0 - 1)$	—
F	Faraday equivalent	$A T M^{-1}$
h	height of fluidized bed	L
h_0	height of still bed	L
i	current density	$A L^{-2}$
i_L	limiting current density	$A L^{-2}$
K_m	conductivity of metal phase	$R^{-1} L^{-1}$
K_s	conductivity of solution phase	$R^{-1} L^{-1}$
k	mass transfer coefficient	$L T^{-1}$
k_p	mass transfer coefficient of particles	$L T^{-1}$
L	bed thickness	L
m	power of Reynolds' number	—
N_i	the total flux of a given ion	$M L^{-2} T^{-1}$
n	number of valences	—
u	solution velocity respect to an empty tube	$L T^{-1}$
u_{mf}	minimum fluidization velocity	$L T^{-1}$
u_T	terminal fluidization velocity	$L T^{-1}$
δ_d	thickness of diffusion sublayer	L
ε	porosity	—
ν	kinematic viscosity of solution	$L^2 T^{-1}$
ϱ_m	specific resistivity of metal phase	$R L$
ϱ_s	specific resistivity of solution phase	$R L$
Φ	potential between solution and electrode $(\Phi = \Phi_s - \Phi_m)$	V
Φ_s	solution potential	V
Φ_m	metal phase potential	U
Re	Reynolds' number	—
Sc	Schmidt's number	—

References

1. BENNION, D. N.: International Society of Electrochem. 27 th. Meeting. No. 69. 1976. Zürich.
2. GOODRIDGE, F.: Chem. and Process. Eng. **49** 93 (1968)
3. IBL, N.: Chem. Ing. Techn. **43** 202 (1971)
4. BECK, F.: Chem. Ing. Techn. **41** 943 (1969)
5. CARBIN, D. C.—GABE, D. R.: Electrochimica Acta **19** 645 (1974)
6. SKELLAND, A. H. P.: Diffusional Mass Transfer p. 109 Wiley, Interscience, New York. 1974
7. BEEK, W. J.: Fluidization (Ed. by Davidson and Harrison) P. 433. Academic Press. London. 1971
8. THOENES, D.—KRAMERS, H.: Chem. Eng. Sci. **8** 271 (1958)
9. KRISHNA, M. S.—JAGANNADHARAJU, G. J. V.—RAO, C. V.: Periodica Polytechn. Chem. Eng. **11** (2) 95 (1967)
10. RAMANA RAO, M. V.—RAO, C. V.: Indian J. Technol. **8** 44 (1970)
11. JOTTRAND, R.—GRUNCHARD, F.: 3rd. Cong. Eur. Fed. Chem. Session B. p. 211. London 1962
12. JAGANNADHARAJU, G. J. V.—RAO, C. V.: Indian J. Technol. **3** 201 (1965)
13. KRISHNA, M. S.—JAGANNADHARAJU, G. J. V.: Indian J. Technol. **4** 8 (1966)
14. COEURET, F.—LE GOFF, P.: Electrochimica Acta **21** 195 (1976)
15. ZIEGLER, E. N.—HOLMES, I. T.: Chem. Eng. Sci. **21** 117 (1966)
16. GOODRIDGE, F.: Techniques of Chemistry, Part I. (Ed. by Weinberg, H. L.) p. 23. Wiley Interscience, 1974
17. BEEK, W. J.: Fluidization (Ed. by Davidson and Harrison) p. 440. Academic Press. London. 1971
18. THOENES, D.—KRAMERS, H.: Chem. Eng. Sci. **8** 271 (1958)
19. CHU, J. C.—KALIL, J.—WETTEROTH, W. A.: Chem. Eng. Progr. **49** (3) 141 (1953)
20. FLEISCHMANN, M.—OLDFIELD, I. W.—PORTER. D. F.: Electroanal. Chem. **29**, 241 (1971)
21. GOODRIDGE, F.—HOLDEN, D. J.—PLIMLEY, R. E.: Trans. Inst. Chem. Engrs. **49**, 137 (1971)
22. ARMSTRONG, R. D.—BROWN, O. R.—GILES, R. D.: Nature **219**, 94 (1968)

dr. László Kovács   H-1521 Budapest